

# IMPROVED ALGORITHM FOR HARMONIC LOAD FLOW SOLUTION IN RADIAL DISTRIBUTION NETWORKS

Farhad Safargholi<sup>1</sup>, Behrooz Vahidi<sup>1\*</sup>, Javad Shokrolahi Moghani<sup>1</sup>

1-Department of Electrical Engineering, Amirkabir University of Technology  
Tehran 1591634311, Iran

\* Corresponding author email: vahidi@aut.ac.ir

**Abstract:** *The aim of this paper is to present an improved algorithm to solve harmonic load flow problem in balanced radial distribution systems with laterals, which have nonlinear load. The method is efficient and easy to implement. This method is iterative and allows the evaluation of both, voltage (rms) values and phase angles of the fundamental voltage and harmonic voltage for each bus. The proposed method in this paper can be solved harmonic load flow problem iteratively from two sets of recursive equations. The first set concern the determination of the branches current by going up the line (backward sweep). The second one allows us to determine the nodes voltage by going down the line (forward sweep). The total harmonic distortion can also be calculated easily.*

**Keywords:** *Harmonic load flow, Radial distribution network, Nonlinear load, THD.*

## 1. INTRODUCTION

Many researchers are used different search algorithms for solving optimization problems in power system [1-6].

Load flow problem has an important role in power system design and analysis. Also, the harmonic load flow is used for small-signal analysis, that is necessary for controller design and stability analysis. Moreover, in the startup a transient program, Initializing variables are important. Those accurate steady-state initializations are received from accurate harmonic load flow [7].

Researchers are proposed a number of harmonic load flow methods [8]. In general, these methods can be divided into three categories:

Time-domain methods [9-15].

Frequency-domain methods [16-24].

Hybrid time–frequency domain methods [25, 26].

The absence of limitation in load flow problem is one of the main disadvantages of the time-domain method (such as active and reactive power demands can be assumed specified constant values) at the fundamental frequency. A time-domain program needs to a harmonic power flow algorithm for the steady-state initialization. In [27], has been presented a time-domain based transient-state analysis that has been utilized the EMPT program for harmonic analysis. Perkins *et al.* [28] have implemented an initialization algorithm based on a time-domain steady-state analysis; that, this method is introduced in ref. [8, 9]. In ref. [9], the nonlinear components are modeled by means of piecewise linearization.

However, most of the harmonic power flow methods are used from the frequency domain [29]. The accuracy of the solution of this method depends on the number of harmonics included in the calculation process. In addition, the number of harmonics also determines the dimensions of the system, which affects the overall simulation time.

Xia and Heydt [16,17] have developed the conventional power flow analysis for harmonic load flow and nonlinear component in the formulation Are considered. However, this method only allows specific harmonics to be taken into account. Researchers have developed this harmonic load flow to three phase networks [23, 30].

Arrillaga *et al.* [14] have represented how modeling of nonlinear component in the three-phase frame of reference in the harmonic load flow. Valcárcel and Mayordomo [31] have solved this problem based on two separate Newton-Raphson equations. That, one of them for the three-phase conventional power flow and the other for calculation the harmonics injected by the nonlinear loads.

This paper presents a new frequency-domain harmonic power-flow algorithm. This algorithm can be used for load flow problem in radial distribution feeders with laterals. In this paper, a simple method for numbering the branches and nodes are used [32]. Then, based on a new algorithm, the matrix of nodes connected to different branches of the network is calculated so that the nodes beyond each branch are determined. Using this matrix and power nodes, the current of branches are calculated. Then the nodes voltage drop at each harmonic can be determined. This process is done for all the harmonics respectively. In this paper, three-phase diode bridge rectifier is modeled, and considered in the analysis of the load flow.

## 2. COMPONENTS MODEL

In an industrial distribution system, the main equipment that needs to be considered in the harmonic analysis is distribution cable, transformer, nonlinear load, capacitor and inductor etc. Instead of using the very accurate model, some practical and approximated models for industrial use are employed in this paper [16, 17 and 22].

### 2.1. Distribution Cable

Some corrections need to be applied to the resistance and the internal inductance of a distribution cable at high frequency and several modifications have been developed to cope with this purpose. However, a simple model is enough for a practical harmonic analysis. If the line impedance of fundamental frequency is given by:

$$Z_L^{(h)} = R_L + jhX_L \quad (1)$$

### 2.2. Three-Phase Rectifier

Many commercial and industrial appliances require direct current for their operation. The three-phase diode bridge rectifier (Fig. 1) has become a popular power source for these appliances because of its reduced cost and relatively low sensitivity to supply voltage variations under normal

operating conditions. But, these converters have been one of the most important elements in the harmonic of grid.

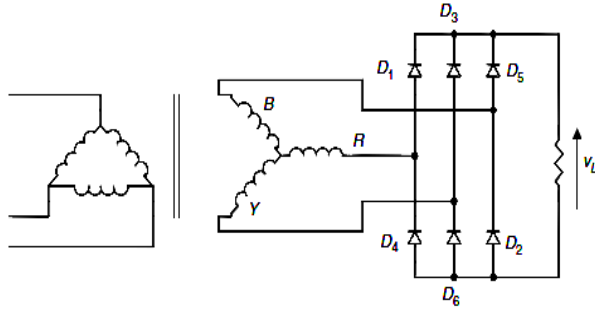


Figure. 1. Three-phase diode bridge rectifier.

A three-phase rectifier is characterized by a very inductive DC side configuration relative to the AC system side. Under these conditions, the DC current is reasonably constant and the converter acts as a source of harmonic voltage on the DC side and of harmonic current on the AC side.

Six-pulse rectification (and inversion) is obtained from three-phase two-way configurations. That, in this rectifier the phase currents consists of periodic positive rectangular pulses of width  $w = 2\pi/3$ , repeating at the supply frequency. The waveform of the phase current is shown in Fig. 2. If the actual DC current be equal to  $I_d$ , then the current in phase  $a$  is [16]:

$$i_a = \frac{2\sqrt{3}}{\pi} I_d (\cos(\omega t) + \frac{1}{5} \cos(5\omega t) - \frac{1}{7} \cos(7\omega t) + \frac{1}{11} \cos(11\omega t) - \frac{1}{13} \cos(13\omega t) + \frac{1}{17} \cos(17\omega t) - \frac{1}{19} \cos(19\omega t) \dots) \quad (2)$$

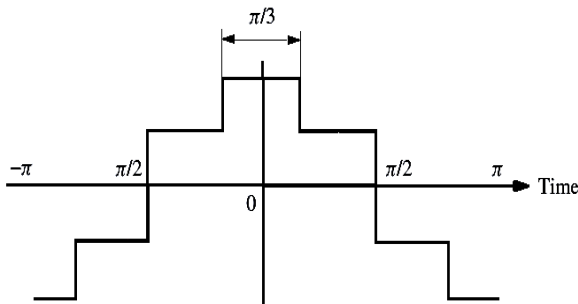


Figure. 2. Time-domain representation of a six-pulse waveform with delta-star transformer.

### 3. NODES LOCATED BEYOND EACH BRANCH

In this paper, a method based on backward and forward sweeps is used for solving the load flow problem in balanced radial distribution systems. A simple method of [32] is used here for numbering the branches and nodes. Using a new algorithm, the nodes are identified beyond each branch of the network as a matrix called *NBEB* matrix.

To identify the nodes beyond each branch (*NBEB*), the following algorithm is used for numbering the nodes and branches [11]. The first bus (source node) is numbered as bus number 0. Buses should be numbered on the main feeder to the end, respectively. Thereafter, the lateral branches following from the nearest lateral branch relative to the source node (if two branches have the same position relative to the reference bus, starting from each one is arbitrary) and then buses following the last bus in the main feeder are respectively numbered. Then, similarly, the buses are numbered at other lateral branches following the last bus at the last lateral branch. Numbering of branches is also similar to the numbering of buses.

The network shown in Fig. 3, presents numbering scheme of buses and branches according to the algorithm. Table 1 lists start and end nodes of each branch.

Fig. 4 shows the proposed algorithm for determining nodes beyond each branch of the network. This algorithm receives the total number of branches, number of the last node in the main feeder, number of lateral branches and number of start and end nodes of each lateral branch. The output of this algorithm is a matrix named *NBEB*. The rows of this matrix correspond to the branch network. For the  $i^{th}$  branch, non-zero values of *NBEB* ( $i, j$ ) are the number of buses beyond the  $i^{th}$  branches ( $M(i)$  is equal to the total number of buses beyond the  $i^{th}$  branch). For example, for the network shown in Fig.1, the following equations can be written:

$$NBEB(3,1) = 3; NBEB(3,2) = 4; NBEB(3,3) = 7$$

$$NBEB(3,4) = 8; M(3) = 4; NBEB(3, j) = 0, j = 4, 5, 6, 7$$

And, the *NBEB* matrix, derived using this method, is as follows:

$$NBEB = \begin{pmatrix} 1 & 2 & 3 & 4 & 5 & 6 & 7 & 8 & 9 & 10 \\ 2 & 3 & 4 & 0 & 6 & 0 & 8 & 0 & 10 & 0 \\ 3 & 4 & 9 & 0 & 0 & 0 & 0 & 0 & 0 & 0 \\ 4 & 5 & 10 & 0 & 0 & 0 & 0 & 0 & 0 & 0 \\ 5 & 6 & 0 & 0 & 0 & 0 & 0 & 0 & 0 & 0 \\ 6 & 7 & 0 & 0 & 0 & 0 & 0 & 0 & 0 & 0 \\ 7 & 8 & 0 & 0 & 0 & 0 & 0 & 0 & 0 & 0 \\ 8 & 9 & 0 & 0 & 0 & 0 & 0 & 0 & 0 & 0 \\ 9 & 10 & 0 & 0 & 0 & 0 & 0 & 0 & 0 & 0 \\ 10 & 0 & 0 & 0 & 0 & 0 & 0 & 0 & 0 & 0 \end{pmatrix}$$

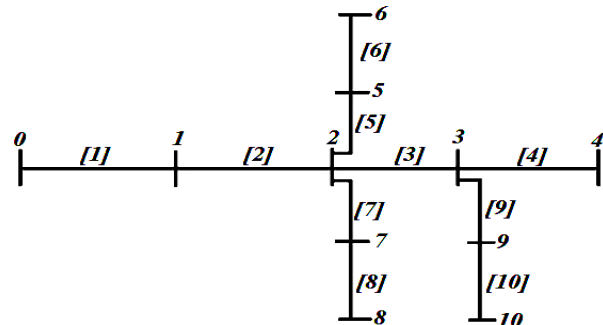


Figure. 3. Nodes and branches numbering scheme.

**TABLE 1.**  
**FEEDER CONNECTIVITY**

Branch	Start node of branch	End node of branch
1	0	1
2	1	2
3	2	3
4	3	4
5	2	5
6	5	6
7	2	7
8	7	8
9	3	9
10	9	10

**4. LOAD FLOW EQUATIONS**

It is assumed that the three-phase radial distribution network is balanced. The load flow of the radial distribution network for any specific harmonic can be solved iteratively by two sets of recursive equations. The first set should determine of the branches current by going up the line (backward sweep). The second one determines the nodes voltage by going down the line (forward sweep).

Consider the  $i^{th}$  branch network. Starting bus of the  $i^{th}$  branch and the end bus of the branch are, respectively, called SE (i) and RE(i) (Power is entered to the branch through starting bus.).

Assume that:  $P_{Load}^{(h)}(k)$  and  $Q_{Load}^{(h)}(k)$  are active and reactive load powers at node k and for  $h^{th}$  harmonic;  $P_{Loss}^{(h)}(k)$  and  $Q_{Loss}^{(h)}(k)$  are active and reactive power losses at the  $k^{th}$  branch and for  $h^{th}$  harmonic. Therefore,  $P^{(h)}(RE(i))$  and  $Q^{(h)}(RE(i))$  are active and reactive powers at the end of the branch i, as follows:

$$P^{(h)}(RE(i)) = \sum_{k=BNC(i,1)}^{BNC(i,M(i))} [P_{Load}^{(h)}(k)] + \sum_{k=BNC(i,2)}^{BNC(i,M(i))} P_{Loss}^{(h)}(k) \tag{3}$$

$$Q^{(h)}(RE(i)) = \sum_{k=BNC(i,1)}^{BNC(i,M(i))} [Q_{Load}^{(h)}(k)] + \sum_{k=BNC(i,2)}^{BNC(i,M(i))} Q_{Loss}^{(h)}(k)$$

By this equation, the  $i^{th}$  branch active and reactive power losses at  $h^{th}$  harmonic are calculated. Therefore, active and reactive powers at the beginning of the  $i^{th}$  branch and for  $h^{th}$  harmonic can be calculated by the following equation:

$$P_{Loss}^{(h)}(i) = \frac{P^{(h)}(RE(i))^2 + Q^{(h)}(RE(i))^2}{|V_i^{(h)}|^2} r_i^{(h)} \tag{4}$$

$$Q_{Loss}^{(h)}(i) = \frac{P^{(h)}(RE(i))^2 + Q^{(h)}(RE(i))^2}{|V_i^{(h)}|^2} x_i^{(h)}$$

$$P^{(h)}(SE(i)) = P^{(h)}(RE(i)) + P_{Loss}^{(h)}(i) \tag{5}$$

$$Q^{(h)}(SE(i)) = Q^{(h)}(RE(i)) + Q_{Loss}^{(h)}(i)$$

where,  $r_i^{(h)}(x_i^{(h)})$  is the resistance (reactance) of the  $i^{th}$  branch and for  $h^{th}$  harmonic.

The current flowing through the  $i^{th}$  branch and for  $h^{th}$  harmonic is given by the following equation:

$$I^{(h)}(i) = \frac{P^{(h)}(SE(i)) - jQ^{(h)}(SE(i))}{V^{(h)}(SE(i))^*} \tag{6}$$

Therefore, the voltage of the bus at the end of the branch (i) is written, as follows:

$$V^{(h)}(RE(i)) = V^{(h)}(SE(i)) - (r_i^{(h)} + jx_i^{(h)})I^{(h)}(i) \tag{7}$$

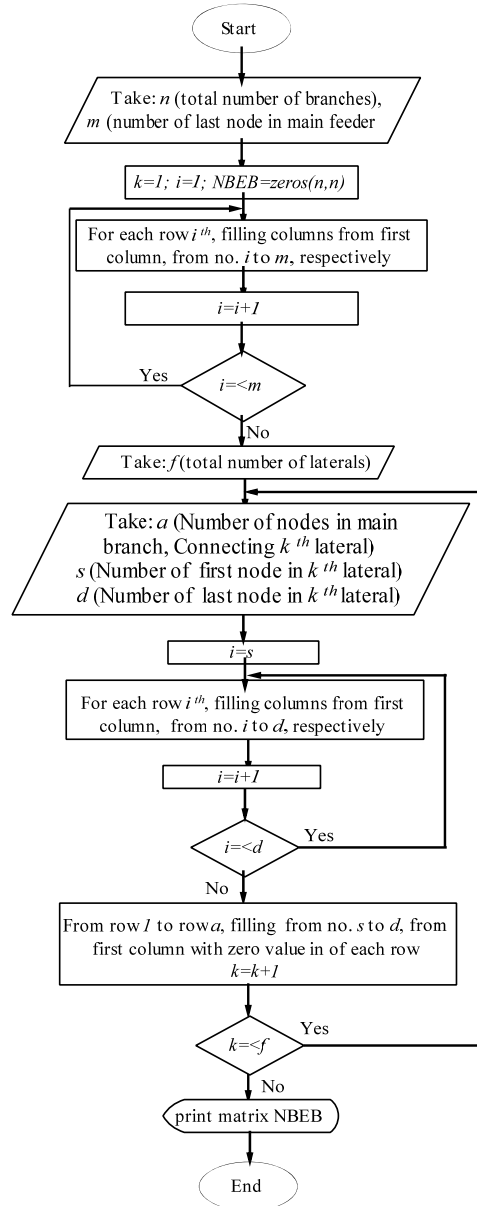


**Figure.4. Node determination after branch (NBEB matrix)**

In this method, the voltage rms value and phase-angle of the reference bus (bus number zero) are considered respectively 1.0 pu. and zero. Also in the first iteration, the voltage rms

value and phase-angle of the all buses are assumed to be, respectively, 1.0 pu. and zero.

**5. DEVELOPED ALGORITHM**

In this paper, a program to solve the load flow problem is developed in MATLAB environment. This program, as shown in Fig.5, receives the load, line and nonlinear load; then it makes matrix NBEB. In next step for the fundamental frequency and any harmonic, starting from the last branch, the crossing active and reactive powers from branch *i* and in the same harmonic according to the equation (3) and power losses at branch *i* and in the same harmonic on the basis of the voltage at the sending end node and according to the equation (4) is calculated. Then the crossing active and reactive powers from branch *i* and in the same harmonic according to the equation (5) is calculated. Then, the current in the branch *i* and in the same harmonic according to (6) on the basis of the voltage at the sending-end node is calculated. In next step, the voltage at the receiving-end node of branch *i* and in the same harmonic, according to (7) is calculated. Then, these steps are repeated for branch *i-1* and the mentioned steps are repeated to achieve the source node. Then, the convergence rate is compared. This process is done for all the harmonics respectively. The effect of three-phase rectifier in the load flow equations has been considered as follows:

In the first step, to calculate the fundamental frequency of bus voltage, the power of rectifier is modeled as a load (Fig. 6). Based on the fundamental voltage and following equation, the current of equivalent load is calculated.

$$I_K^{(1)} = \frac{P_K}{V_k^{(1)}} \tag{8}$$

So that, according to equation (2) the harmonic components in the other harmonics can be achieved. And in the next step power of any non-linear load in each harmonic Proportional to component harmonic can be obtained.

**6. SIMULATION RESULTS**

The proposed method was tested in the 33-bus system [33] shown in Fig. 7. In this example, the base values are 2300 kVA and 12.66 kV. This case contains a three-phase diode bridge rectifier at the node 17 that its Active power consumption is 150 KW. This rectifier consists of harmonic components based on that the harmonics can be modeled as a constant current load. This value of the harmonic components based on Equation 2, are a multiple of the fundamental current. Then, based on load flow equations, at the first stage, fundamental voltage of each bus and current equivalent to each load are calculated. In the next stage, for each harmonic based on the fundamental current, amount of load at each harmonic is calculated. Then, based on load flow algorithms (shown in Fig. 5), the harmonic voltage at each bus is determined. This process is done for all the harmonics respectively.

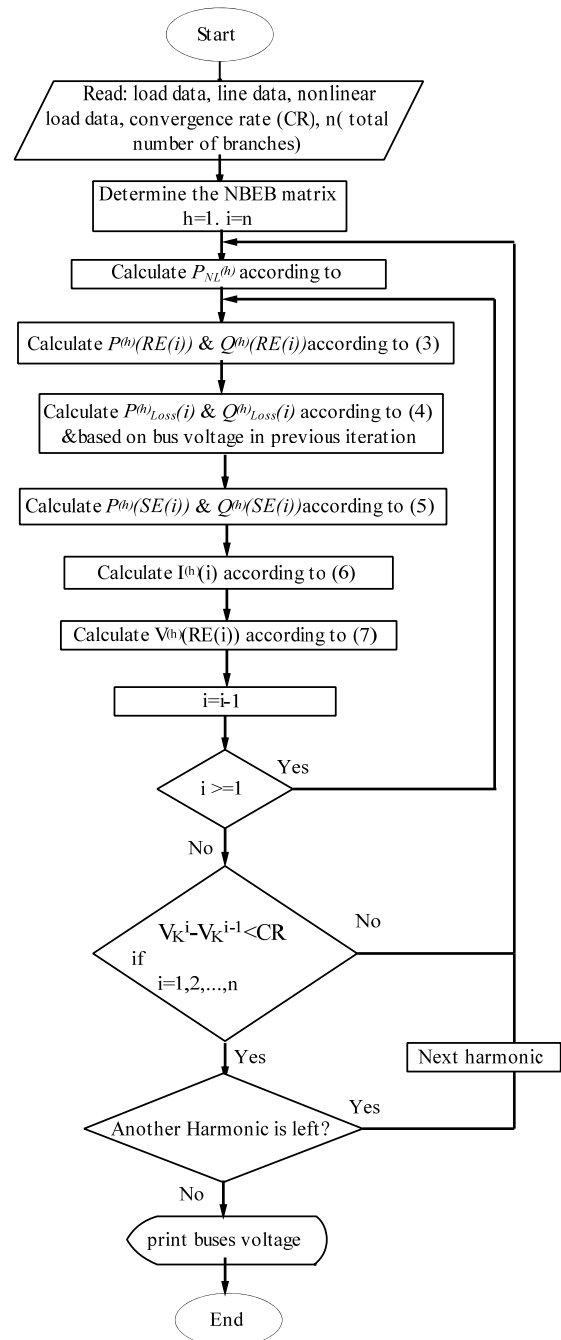


Figure 5. Algorithms of harmonic load flow solution.

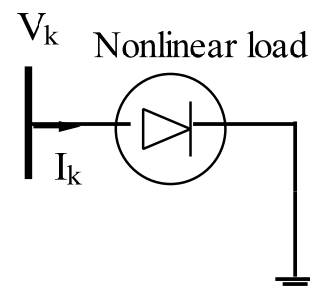
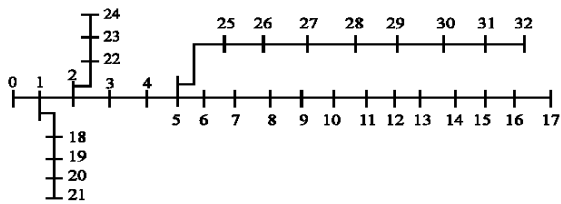


Figure 6. Modeling of nonlinear load for linear analyze.

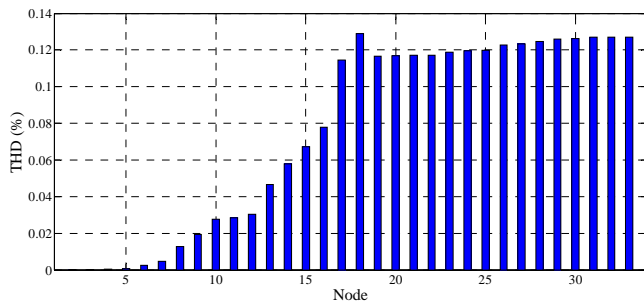
**TABLE 2.**  
**RESULT OF HARMONIC LOAD FLOW**

Node No.	Bus Voltages (p.u)							THD %
	Fund	5 <sup>th</sup>	7 <sup>th</sup>	11 <sup>th</sup>	13 <sup>th</sup>	17 <sup>th</sup>	19 <sup>th</sup>	
0	1	0	0	0	0	0	0	0
1	0.996915	8.867e-05	7.6089e-05	6.4644e-6	6.1567e-5	5.7581e-5	5.6218e-5	2.8581e-6
2	0.982256	0.0005569	0.00047765	4.0559e-5	0.0003862	0.0003611	0.0003525	0.000114
3	0.974357	0.0009045	0.00077575	6.5869e-5	0.0006272	0.0005864	0.0005725	0.000303
4	0.966526	0.0012664	0.00108616	9.2224e-5	0.0008781	0.0008210	0.0008015	0.000600
5	0.947163	0.0024783	0.00214074	0.0001833	0.0017513	0.0016444	0.0016078	0.002411
6	0.943436	0.0034399	0.00299296	0.0002586	0.0024773	0.0023358	0.0022874	0.004796
7	0.937814	0.0056094	0.00487274	0.0004202	0.0040228	0.0037896	0.0037098	0.012750
8	0.930403	0.0069101	0.00599961	0.0005171	0.0049491	0.0046608	0.0045622	0.019465
9	0.923459	0.0082127	0.00712779	0.0006141	0.0058762	0.0055327	0.0054151	0.027661
10	0.922391	0.0083468	0.00724096	0.0006235	0.0059652	0.0056150	0.0054952	0.028555
11	0.920495	0.0086022	0.00745649	0.0006414	0.0061347	0.0057719	0.0056478	0.030297
12	0.912789	0.0106062	0.00919661	0.0007915	0.0075704	0.0071241	0.0069714	0.046506
13	0.909945	0.0117748	0.01022193	0.0008810	0.0084304	0.0079386	0.0077704	0.057760
14	0.907923	0.0126729	0.01100402	0.0009486	0.0090786	0.0085501	0.0083694	0.067113
15	0.905796	0.0136285	0.01183225	0.0010199	0.0097599	0.0091911	0.0089966	0.077760
16	0.902445	0.0164462	0.01430492	0.0012358	0.0118345	0.0111565	0.0109245	0.114472
17	0.901122	0.0174424	0.01516999	0.0013104	0.0125482	0.0118286	0.0115824	0.128900
18	0.996387	0.0174424	0.01516999	0.0013104	0.0125482	0.0118286	0.0115824	0.116576
19	0.992809	0.0174424	0.01516999	0.0013104	0.0125482	0.0118286	0.0115824	0.116996
20	0.992104	0.0174424	0.01516999	0.0013104	0.0125482	0.0118286	0.0115824	0.117079
21	0.991467	0.0174424	0.01516999	0.0013104	0.0125482	0.0118286	0.0115824	0.117155
22	0.978668	0.0174424	0.01516999	0.0013104	0.0125482	0.0118286	0.0115824	0.118687
23	0.971992	0.0174424	0.01516999	0.0013104	0.0125482	0.0118286	0.0115824	0.119502
24	0.968665	0.0174424	0.01516999	0.0013104	0.0125482	0.0118286	0.0115824	0.119912
25	0.945229	0.0174424	0.01516999	0.0013104	0.0125482	0.0118286	0.0115824	0.122885
26	0.942660	0.0174424	0.01516999	0.0013104	0.0125482	0.0118286	0.0115824	0.123220
27	0.931190	0.0174424	0.01516999	0.0013104	0.0125482	0.0118286	0.0115824	0.124738
28	0.922953	0.0174424	0.01516999	0.0013104	0.0125482	0.0118286	0.0115824	0.125851
29	0.919390	0.0174424	0.01516999	0.0013104	0.0125482	0.0118286	0.0115824	0.126339
30	0.915224	0.0174424	0.01516999	0.0013104	0.0125482	0.0118286	0.0115824	0.126914
31	0.914318	0.0174423	0.01516999	0.0013104	0.0125482	0.0118286	0.0115824	0.127039
32	0.914048	0.0174423	0.01516999	0.0013104	0.0125482	0.0118286	0.0115824	0.127076



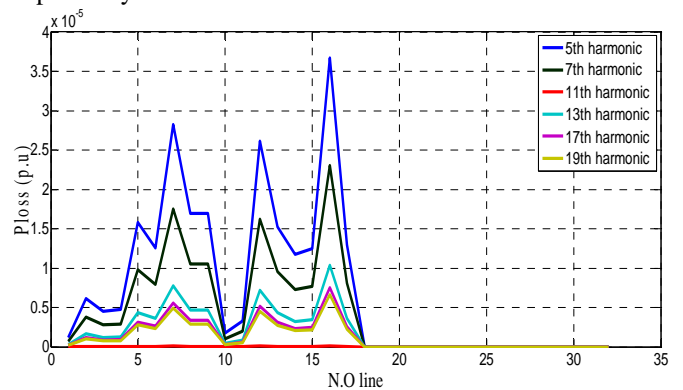
**Figure 7. 33-bus single line diagram.**

Table 2 is shown test results of the system including the fundamental bus voltage, harmonic voltage and THD (%) for each bus and harmonic orders and this diagram is plotted in Fig.8.



**Figure 8. THD (%) for each bus of 33-bus network.**

Active and reactive power losses for each line and harmonic orders in this network is shown in Fig.9 and Fig.10, respectively.



**Figure 9. Active and power losses for each line and harmonic orders.**

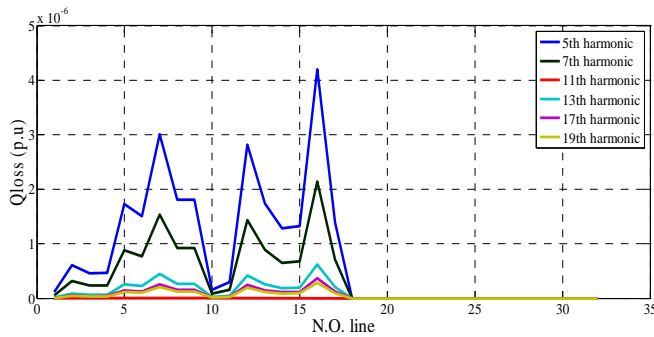


Figure 10. Reactive and power losses for each line and harmonic orders.

## 7. CONCLUSION

In this paper, a time-domain harmonic power-flow method is described for steady-state analysis and is developed a new algorithm for calculating the harmonic voltages in a radial distribution network. This method can be easily extended to three-phase networks. This method allows the evaluation of both, voltage (rms) values and phase angles of the fundamental voltage and harmonic voltage for each bus. The proposed load flow algorithm is easy understanding and acceptable computational performance. Also, one of the most important advantages of this method is that it avoids constructing and inverting any network matrix.

## REFERENCES

- [1] Baghaee, H. R. Jannati, M. Vahidi, B. Hosseinian, S. H. Rastegar, H. "Improvement of voltage stability and reduce power system losses by optimal GA-based allocation of multi-type FACTS devices", 11th International Conference on Optimization of Electrical and Electronic Equipment (11<sup>th</sup> OPTIM), (2008).
- [2] Jazebi, S. Vahidi, B., Jannati, M. "A novel application of wavelet based SVM to transient phenomena identification of power transformers", *Energy Conversion and Management*, **52**: 1354-1363 (2011).
- [3] Baghaee, H. R. Jannati, M. Vahidi, B. Hosseinian, S. H. Jazebi, S., "Optimal multi-type FACTS allocation using genetic algorithm to improve power system security", 12<sup>th</sup> International Middle East Power System Conference, MEPCON, 2008.
- [4] Baghaee, H. R. Jannati, M. Vahidi, B. Hosseinian, S. H. Rastegar, H., "Improvement of voltage stability and reduce power system losses by optimal GA-based allocation of multi type FACTS devices", 11 International Conference on Optimization of Electrical and Electronic Equipment, OPTIM, 2008.
- [5] Jazebi, S. Vahidi, B., "Reconfiguration of distribution networks to mitigate utilities power quality disturbances", *Electric Power System Research*, **91**: 9-17 (2012).
- [6] Jazebi, S. Hosseinian, S. H. Vahidi, B., "A novel approach to adaptive single phase autoreclosure scheme for EHV power transmission lines based on learning error function of ADALINE", *Simulation*, **84**(12): 601-610 (2008).
- [7] Kuo Lung, L. Noda, T., "A time-domain harmonic power-flow algorithm for obtaining nonsinusoidal steady-state solutions", *Power Delivery, IEEE Transactions on*, **25**: 1888-1898 (2010).
- [8] Task Force on Harmonics Modeling and Simulation, "IEEE tutorial course on harmonics and simulation", *IEEE Power Eng. Soc.*, Jun. 2007, Course text 07TP184.
- [9] Aprille, T. J. Trick, T. N., "Steady-state of nonlinear circuits with periodic inputs", *Proc. IEEE*, **60**(1): 108-114 (1972).
- [10] Trick, T. N. F. Colon, F. R. Fan, S. P., "Computation of capacitor voltage and inductor current sensitivities with respect to initial conditions for the steady-state analysis of nonlinear periodic circuits", *IEEE Trans., Circuits Syst.*, **22**(5): 391-396 (1975).
- [11] Segundo, J. Medina, A., "Periodic steady state solution of electric systems including UPFCs by extrapolation to the limit cycle", *IEEE Trans. Power Del.*, **23**(3): 1506-1512 (2008).
- [12] Medina, A., "Harmonic simulation techniques (methods & algorithms)", in *Proc. IEEE Power Eng. Soc. General Meeting*, **1**: 762-765 (2004).
- [13] Femia, N. Spagnuolo, G. Vitelli, M., "Steady-state analysis of PWM dc-to-dc regulators", *IEEE Trans. Aerosp. Electron. Syst.*, **39**(1): 318-334 (2003).
- [14] Garcia, N. Medina, A., "Swift time domain solution of electric systems including SVSs", *IEEE Trans. Power Del.*, **18**(3): 921-927 (2003).
- [15] Medina, A. Garcia, N., "Fast time domain computation of the periodic steady-state of systems with nonlinear and time-varying components", *Elect. Power Energy Syst.*, **26**: 637-640 (2004).
- [16] Xia, D. Heydt, G. T., "Harmonic power flow studies Part I—Formulation and solution", *IEEE Trans. Power App. Syst.*, **PAS-101**(6): 1257-1265 (1982).
- [17] Xia, D. Heydt, G. T., "Harmonic power flow studies Part II—Implementation and practical application", *IEEE Trans. Power App. Syst.*, **PAS-101**(6): 1266-1270 (1982).
- [18] Arrillaga, J. Callaghan, C. D., "Three phase AC-DC load and harmonic flows", *IEEE Trans. Power Del.*, **6**(1): 238-244 (1991).
- [19] Xu, W. Marti, J. R. Dommel, H. W., "A multiphase harmonic load flow solution technique", *IEEE Trans. Power Del.*, **6**(1): 174-182 (1991).
- [20] Arrillaga, J. Medina, A. Lisboa, M. L. V. Cavia, M. A. Sánchez, P., "The harmonic domain. A frame of reference for power system harmonic analysis", *IEEE Trans. Power Syst.*, **10**(1): 433-440 (1995).
- [21] Smith, B. C. Watson, N. R. Wood, A. R. Arrillaga, J., "A Newton solution for the harmonic phasor analysis of ac/dc converters", *IEEE Trans. Power Del.*, **11**(2): 965-971 (1996).
- [22] Arrillaga, J. Smith, B. C. Watson, N. R. Wood, A., *Power Systems Harmonics Analysis*. New York: Wiley, 1997.
- [23] Smith, B. C. Arrillaga, J. Wood, A. R. Watson, N. R., "A review of iterative harmonic analysis for ac-dc

- power systems”, *IEEE Trans. Power Del.*, **13**(1): 180–185 (1998).
- [24] Smith, B. C. Arrillaga, J., “Power flow constrained harmonic analysis in ac-dc power systems”, *IEEE Trans. Power Syst.*, **14**(4): 1251–1261 (1999).
- [25] Semlyen, A. Medina, A., “Computation of the periodic steady state in systems with nonlinear components using a hybrid time and frequency domain methodology”, *IEEE Trans. Power Syst.*, **10**(3): 1498–1504 (1995).
- [26] Semlyen, A. Shlash, M., “Principles of modular harmonic power flow methodology”, *Proc. Inst. Elect. Eng., Gen., Transm. Distrib.*, **147**(1): 1–6 (2000).
- [27] Kitchin, R. H., “Converter Harmonics in Power System Using State-Variable Analysis”, *IEE Proc. Part C*, **128**(4): 567-572 (1981).
- [28] Perkins, B. K. Marti, J. R. Dommel, H. W., “Nonlinear elements in the EMTP: Steady-state initialization”, *IEEE Trans. Power Syst.*, **10**(2): 593–660 (1995).
- [29] Moreno, M. A. de Saá, L. García, J. U., “Three-phase harmonic load flow in frequency and time domains”, *Proc. Inst. Elect. Eng.*, **150**(3): 295–300 (2003).
- [30] Herraiz, S. Sainz, L. Clua, J., “Review of harmonic load flow formulations”, *IEEE Trans. Power Del.*, **18**(3): 1079–1087 (2003).
- [31] Valcárcel, M. Mayordomo, J., “Harmonic power flow for unbalanced systems”, *IEEE Trans. Power Del.*, **8**(4): 2052–2059 (1993).
- [32] Ranjan, R. Venkatesh, B. Das, D., “Voltage stability analysis of radial distribution networks”, *Electric Power Components and Systems*, **31**: 501-511 (2003).
- [33] Taher, S. A. Karimian, A. Hasani, M., “A new method for optimal location and sizing of capacitors in distorted distribution networks using PSO algorithm”, *Simulation Modelling Practice and Theory*, **19**: 662-672 (2011).